HHS Public Access

Author manuscript

Exp Neurol. Author manuscript; available in PMC 2015 March 02.

Published in final edited form as:

Exp Neurol. 2011 March ; 228(1): 80–90. doi:10.1016/j.expneurol.2010.12.011.

Dysfunctions in Circadian Behavior and Physiology in Mouse Models of Huntington's Disease

Takashi Kudo, **Analyne Schroeder**, **Dawn H. Loh**, **Dika Kuljis**, **Maria C. Jordan**[1], **Kenneth P. Roos**[1], and **Christopher S. Colwell**

Department of Psychiatry & Biobehavioral Sciences, University of California - Los Angeles, Los Angeles, CA 90024, USA

[1] Physiology and Cardiovascular Research Lab, University of California, Los Angeles, CA, USA

Abstract

Many patients with Huntington's disease (HD) exhibit disturbances in their daily cycle of sleep and wake as part of their symptoms. These patients have difficulty sleeping at night and staying awake during the day, which has a profound impact on the quality of life of the patients and their care-givers. In the present study, we examined diurnal and circadian rhythms of four models of HD including the BACHD, CAG 140 knock-in and R6/2 CAG 140 and R6/2 CAG 250 lines of mice. The BACHD and both R6/2 lines showed profound circadian phenotypes as measured by wheel-running activity. Focusing on the BACHD line for further analysis, the amplitude of the rhythms in the BACHD mice declined progressively with age. In addition, the circadian regulation of heart rate and body temperature in freely behaving BACHD mice were also disrupted. Furthermore, the distribution of sleep as well as the autonomic regulation of heart rate was disrupted in this HD model. To better understand the mechanistic underpinnings of the circadian disruption, we used electrophysiological tools to record from neurons within the central clock in the suprachiasmatic nucleus (SCN). The BACHD mice exhibit reduced rhythms in spontaneous electrical activity in SCN neurons. Interestingly, the expression of the clock gene PERIOD2 was not altered in the SCN of the BACHD line. Together, this data is consistent with the hypothesis that the HD mutations interfere with the expression of robust circadian rhythms in behavior and physiology. The data raise the possibility that the electrical activity within the central clock itself may be altered in this disease.

Keywords

autonomic nervous system; circadian rhythm; heart rate; Huntington's disease; mouse models of HD; BACHD; R6/2; sleep; suprachiasmatic nucleus

Correspondence to: C. S. Colwell, ccolwell@mednet.ucla.edu.

Author Contributions: TK, AS, DHL and CSC designed the experiments and prepared the manuscript. TK and DHL performed and analyzed the behavioral studies. AS, MCJ, and KPR performed and analyzed the measurements of heart rate and body temperature. TK and DK performed the electrophysiological recordings and IHC experiments. All authors approved the final manuscript.

Introduction

Many patients with Huntington's disease (HD) exhibit disturbances in their daily cycle of sleep and wake as part of their symptoms. These patients have difficulty sleeping at night and staying awake during the day. This dysfunction in timing may not be causal to their disorder, yet these symptoms have a major impact on the quality of life of the patient population and on the family members who care for the HD patients. Previous work has found that a mouse model of HD (R6/2 CAG 245) exhibits a progressive breakdown of their circadian rest/ activity cycle that mimics the condition of human patients typified by: loss of consolidated sleep, increased wakeful activity during the sleep phase, and greater sleep during the active, waking phase (Morton, et al., 2005, Pallier, et al., 2007). This behavioral impairment in the mice is accompanied by disordered expression of circadian clock genes *in vivo* in the master circadian pacemaker in the hypothalamus: the suprachiasmatic nucleus (SCN), and in the motor control regions of the brain, including the striatum. Importantly, the use of hypnotics or scheduled feeding can improve the performance of the R6/2 mice (Maywood, et al., 2010, Pallier, et al., 2007). This work raises the possibility that targeted interventions to improve daily rhythms in patients may improve clinical symptoms of HD. HD is caused by an expanded CAG repeat in the huntingtin (HTT) protein (The Huntington's Disease Collaborative Research Group, 1993). There are 3 general types of mouse models of HD, including transgenic mice expressing the entire human *HTT* gene with 97 mixed CAA-CAG repeats (BACHD), as well as models expressing the first exon of the *HTT* gene with varying lengths of the CAG repeats (R6/2). Finally, there are knock-in mice generated by inserting a 140 CAG repeat expansion into the mouse *Htt* gene (CAG 140 knock-in). No single mouse model can be expected to recapitulate all aspects of the human disease, and we hence felt that it was important to explore possible circadian dysfunction in different mouse models of HD.

In the present study, we first sought to determine whether circadian rhythms in wheel running activity are disrupted in four mouse models of HD: BACHD (Gray, et al., 2008), CAG 140 knock-in (Menalled, et al., 2003), R6/2 with 140 CAG repeats, and R6/2 with 250 CAG repeats (Mangiarini, et al., 1996) lines of mice. These mouse lines were screened by monitoring daily rhythms of wheel-running activity. This simple and automated assay is the method of choice for screening mutations that influence the circadian system of mammals. Due to the relatively short lifespan of the two R6/2 lines, we focused on the BACHD line for further long-term analysis using radiotelemetry in order to examine rhythms in heart rate and body temperature from freely behaving mice. We also specifically evaluated the possibility of alterations in autonomic regulation of heart rate in the BACHD model. Next, we sought to determine whether the BACHD mice exhibit reduced rhythms in spontaneous electrical firing in the SCN. Finally, we examined the daily rhythms of clock gene expression in the SCN of the BACHD mice. Together, these experiments examine the impact of the mutations causing HD on circadian behavior and provide the beginnings of a mechanistic understanding of how the HD mutation alters the physiological properties of the circadian timing system.

Material and methods

Animals

The experimental protocols used in this study were approved by the UCLA Animal Research Committee and all recommendations for animal use and welfare, as dictated by the UCLA Division of Laboratory Animals and the guidelines from the National Institutes of Health, were followed. We used four lines of mice in this study: BACHD on the C57BL6/J background (Gray, et al., 2008), CAG 140 knock-in (KI) originally on a C57BL/6J x 129/Sv background, now N2-N3 on the C57BL/6J background (Hickey, et al., 2008, Menalled, et al., 2003), and the R6/2 CAG 140 and R6/2 CAG 250 on the C57BL/6J background (Mangiarini, et al., 1996). The transgene insertion site for the R6/2 and BACHD lines have not been characterized, and potential positional effects cannot currently be ruled out. The BACHD and both R6/2 lines were fully backcrossed into the C57BL/6J strain. Mutants and littermate wild-type (WT) controls were obtained from the mouse mutant resource at JAX (The Jackson Laboratory, Bar Harbor, Maine) in a colony maintained by the CHDI Foundation. For each line, we studied littermate mutants and WT controls in parallel. Genotype was determined at 15 days of age by PCR of tail snips. For the R6/2 and CAG 140 KI lines, the CAG repeat lengths were measured by Laragen (Los Angeles, CA). The mice were inspected daily for signs of ill health and euthanized if necessary.

Behavioral analysis

Methods employed were similar to those described previously (Colwell, et al., 2003, Colwell, et al., 2004). Male mice, at least 1 month (mo) of age, were housed individually and their wheel-running activity recorded as revolutions (rev) per 3 min interval. The running wheels and data acquisition system were obtained from Mini Mitter Co. (Bend, OR). The animals were exposed to a 12:12 light-dark cycle (LD; light intensity 300 Lux) for two weeks. For some mice, the LD cycle was shifted 6 hrs earlier or 6 hrs later and the number of cycle required for re-synchronization measured. The animals were then placed into constant darkness (DD) to assess their free-running activity pattern. The locomotor activity rhythms of mice were analyzed by periodogram analysis combined with the χ^2 test with $P = 0.05$ significance level (El Temps, Barcelona, Spain) on the raw data. The periodogram shows the amplitude (referred to as “power”) of periodicities in the time series for all periods of interest (between 20 and 31 h in 3 min steps). The power values were normalized to the percentage of variance derived from the Qp values of the periodogram (Qp x 100/N; N = total number of data points) according to the calculated $P = 0.05$ significance level. Slopes of an eye-fitted line through the onsets were also used to confirm period 5 estimates made with the periodogram analysis. The average pattern of activity (i.e. the waveform estimate) was also determined at modulo-period for each animal in DD for 15 cycles. Some mice in DD were exposed to a brief light treatment at circadian time (CT) 16 with CT 12 defined by the locomotor activity onset. Following each treatment, the animals were allowed to free-run undisturbed in DD for 14 days. The light stimulus that was used to induce phase shifts was an exposure to white light (100 Lux, 10 min). Phase shifts in the activity rhythm were determined by measuring the phase difference between eye-fitted lines connecting the onset of activity for a period of 10 days before and 10 days after an experimental manipulation. Measurements were made by investigators “blind” to the

experimental group. In order to estimate the steady state phase delays produced, one day of data after treatments were excluded from the analysis. Stimulus intensity (Lux) was measured with a light meter (BK precision, Yorba Linda, CA). All handling of animals was carried out either in the light portion of the LD cycle or in DD with the aid of night vision goggles (FJW Industries, Palatine, IL).

Sleep measurements

BACHD mutants and their WT littermates were first entrained to a 12:12 LD cycle for at least 2 weeks. The mice were housed individually in the absence of wheels and recorded using a video surveillance camera system (Gadspot, GS-335C, City of Industry, CA). The sleep state is marked by several easily observed behaviors, including adoption of a species-specific sleep posture with the eyes closed (Campbell and Tobler, 1984). We scored a mouse as being asleep only when its eyes were closed as it lay on its side, or if it was curled up with its head tucked into its body, or if the mouse did not make any movements other than brief transitional changes in posture for durations of at least 40 sec. We and others have previously employed this method to determine the basic temporal distribution of behavioral sleep across a 24-h period (Loh, et al., 2010, Pack, et al., 2007, Schwartz and Smale, 2005). Sleep/wake behavior was scored visually in 5 min intervals, which were summed and averaged to determine day and night percentages of time spent in sleep. Consolidation was determined by counting the number of consecutive bins of sleep that exceeded 20 min in duration.

Telemetry Measurements

Methods employed were similar to those described previously (Schroeder, et al., 2010). WT and BACHD mice (4-5 mo) were surgically implanted with a wireless radio-frequency transmitter (ETA-F20, Data Sciences International, St. Paul, MN). Mice were housed in individual cages in the absence of a running wheel. Cages were placed atop telemetry receivers (Data Sciences International) in a light and temperature-controlled chamber. Standard rodent chow was provided *ad libitum*. Data collection began 2 weeks post-surgery, to allow mice to recover in the 12:12 LD cycle. We recorded 20 sec of electrocardiogram (ECG) and measured average body temperature and cage activity every 10 min for approximately 15 days. Similar to our collection of wheel-running behavior, we then shifted the mice into DD and continued the measurements for another 15-20 days. Heart rate (HR) is extrapolated from ECG waveforms using the RR interval.

ECG interval measurements (RR, PR, QRS, QT and QTc) were calculated using Ponemah Analysis Software (Data Sciences International) at time points zeitgeber time (ZT) 2-4 and ZT 14-16 (LD conditions). A 20 sec ECG recording every hr was used to calculate Heart Rate Variability (HRV) in the time-domain (standard deviation of all normal R-R intervals, SDNN) using analysis software (Data Science International). Circadian rhythms of HR and body temperature were analyzed by periodogram analysis combined with a χ^2 test (El Temps software, Barcelona, Spain). The strongest amplitude (or power) of periodicities (within 20 and 31 hr limits) was compared between WT and BACHD deficient mice. The amplitude of the χ^2 test determines the period of a rhythm and its robustness.

Whole cell patch-clamp electrophysiology

Methods used were similar to those described previously (Itri, et al., 2005, Itri, et al., 2009). 300 μm coronal slices of the mid-SCN were collected by vibratome dissection of brains from mice between 2 and 3 months of age. Slices were placed in a recording chamber (PH-1, Warner Instruments, Hamden, CT) attached to the stage of a fixed-stage upright DIC microscope (OLYMPUS, Tokyo, Japan). The slices were superfused continuously (2 ml/min) with artificial cerebrospinal fluid (ACSF) aerated with 95 % O_2/ 5 % CO_2. The whole cell patch clamp recordings from the SCN were taken with recording electrodes. These micropipettes (typically 4–7 MΩ) were pulled from glass capillaries (WPI, Sarasota, FL) on a multistage puller (Sutter P-97, Novato, CA) and filled with the standard solution. The standard solution contained (in mM): K-gluconate, 112.5; EGTA, 1; Hepes, 10; MgATP, 5; GTP, 1; leupeptin, 0.1; phosphocreatine, 10; NaCl, 4; KCl, 17.5; CaCl2, 0.5; and MgCl2, 1. The pH was adjusted to 7.25-7.3 and the osmolality was adjusted between 290-300 mOsm. Recordings were obtained with AXOPATCH 200B amplifier (Molecular Devices, Sunnyvale, CA) and monitored online with pCLAMP (Ver 9.2, Molecular Devices). To minimize changes in offset potentials with changing ionic conditions, the ground path used a KCl agar bridge. Each of the cells was determined to be within the SCN by directly visualizing the cell's location with DIC microscopy. Cells were approached with slight positive pressure (2–3 cm H_2O). The pipette was lowered to the vicinity of the membrane while maintaining positive pressure. After forming a high-resistance seal (2–10 GΩ) by applying negative pressure, a second pulse of negative pressure was used to break the membrane. The access resistance of these cells ranged from 15-35 MΩ in the whole cell voltage-clamp configuration while the cell capacitance was typically between 6-18 pF. Data were not collected if access resistance was greater than 40 MΩ or if the value changed significantly (>20%) during the course of the experiment. In these studies, we used a 70% compensation using positive feedback correction. The junction potentials between the pipette and the extracellular solution were cancelled by the voltage-offset of the amplifier before establishing a seal and were not further corrected. Series and input resistance were monitored repeatedly by checking the response to small pulses in a passive potential range. The standard extracellular solution used for all experiments was ACSF. Drug treatments were performed by dissolving pharmacological agents in the ACSF used to bathe the slices during recording. Solution exchanges within the slice were achieved by a rapid gravity feed delivery system. Spontaneous firing rates (SFR) were recorded with pCLAMP for 1 min using current-clamp in the whole cell patch configuration. No current was injected during recording.

Immunohistochemistry (IHC)

The methods employed were similar to those previously described (Dragich, et al., 2010, Wang, et al., 2009). BACHD and WT littermates of 12 mo of age were used. Mice were anaesthetized by Isoflurane (Phoenix Pharmaceutical, Burlingame, CA) and perfused with phosphate-buffered saline **(**PBS, pH 7.4) with heparin (2 units/ml, Henry Schein, Melville, NY) followed by 4% (w/v) paraformaldehyde (Sigma-Aldrich) in PBS (pH 7.4). Brains were dissected, post-fixed at 4 °C overnight, and cryoprotected in 20 % sucrose in PBS (pH 7.4). IHC was performed on free-floating 20 μm cryostat (Thermo Fisher Scientific,

Waltham, MA) coronal brain sections from the middle of the rostral-caudal axis. Sections were washed for 5 min with PBS (pH 7.4, three times), and then endogenous peroxidase activity was quenched with PBS (3 % H_2O_2, 10 % Methanol, 10 min). Sections were then washed again in PBS (three times), dipped in 3 % normal goat serum in PBS with 0.1 % Triton X-100 for 1 hr, and then incubated with a rabbit anti-PER2 (1:1,000; Alpha Diagnostics, San Antonio, TX) in PBS (3 % normal goat serum, 0.1 % Triton X-100) at 4 °C overnight. Sections were washed in PBS (three times), then incubated with biotinylated goat anti-rabbit antibody (1:200) for 2 hr. Sections were washed again for 5 min in PBS (five times) and dipped in AB solution (Vector Laboratories, Burlingame, CA) for 45 min, washed again in PBS (three times), then placed in filtered 0.05 % 3,3'-diaminobenzidine in Tris-buffered saline (TBS) containing a 1:800 dilution of 1.3 % H_2O_2. After sufficient color reaction (5-6 min), sections were washed with TBS and mounted on slides immediately. Sections were then dried overnight, dehydrated with ascending concentrations of ethanol, and cover-slipped. Images were captured with Axio Vision camera systems (Carl Zeiss, Thornwood, NY). Control experiments in which the primary antibody was not added did not exhibit any positive staining. In addition, blocking experiments, performed by adding the PER2 peptide (1 mg/ml in PBS, pH 7.4, diluted 1:500) to the primary incubation solution, prevented PER2 staining. In previous work using the same protocol, we could not detect any positive staining in PER2 KO mouse (Wang et al., 2009).

Statistical measurements

The data sets were analyzed by a two-way analysis of variance (ANOVA) or a one-way ANOVA. If significant group differences were detected ($P < 0.05$) by the ANOVA, then the post hoc analysis was applied. If the data passed an equal variance test, Tukey's method was applied and if the data failed an equal variance test, Holm-Sidak method was applied. For all tests, values were considered significantly different if $P < 0.05$. All tests were performed using SigmaStat (version 3.5, SYSTAT Software, San Jose, CA). Values were shown as mean ± standard error of the mean (S.E.M.).

Results

Diurnal and circadian rhythms of wheel running behavior are disrupted in R6/2 and BACHD mouse models of HD

We used wheel-running activity to determine the impact of the insertion of the different *Htt/HTT* mutations on diurnal and circadian rhythms of behavior (**Fig. 1**). In these studies, we compared locomotor activity rhythms in WT mice to locomotor activity measured in littermate BACHD ($n = 8$), R6/2 CAG 250 ($n = 5$), R6/2 CAG 140 ($n = 7$), and CAG 140 KI ($n = 8$) lines of mice at 2 to 3 mo of age. As has been previously described (Morton, et al., 2005), under both LD and DD conditions, the majority of mice from the R6/2 lines were arrhythmic (**Table 1**). Due to mortality, we were not able to study the R6/2 lines past this time point. In contrast to the results obtained with the R6/2 lines, the CAG 140 KI remained robustly rhythmic at this age (~3 mo). In fact, this line showed no significant deficits in the key circadian parameters of period or amplitude even when we extended our analysis up to 12 mo of age (data not shown). The BACHD mice (8 out of 8) exhibited low amplitude, fragmented rhythms in wheel running behavior with a long free-running period (**Table 1**). In

addition, most of the BACHD mice exhibited a bimodal activity pattern (75%). These circadian deficits were seen throughout the first year of life of these mice (**Fig. 2**). The amplitude of the rhythms in both LD and DD progressively declined over the life of the mice (**Table 2**). For example, analysis of activity in DD by two-way ANOVA for age and genotype revealed a significant effect of both age ($F_{3,40} = 3.48$, $P = 0.02$) and genotype ($F_{1,40} = 43.38$, $P < 0.001$) with a post hoc Tukey's test indicating a significant effect of the BACHD mutation in all age groups. Together, our behavioral analysis demonstrates that by three mo of age (young adult), three mouse models of HD (BACHD, R6/2 CAG 250, & R6/2 CAG 140) exhibit disrupted daily and circadian rhythms in wheel-running activity.

The light-response of the circadian system is altered in BACHD mice

As nocturnal animals, WT mice restrict most of their wheel running activity to the night (93% of total activity). In contrast, the BACHD mice exhibited a significant amount of wheel running activity in the light (24%; $t_{14} = -3.54$, $P < 0.001$). One possible explanation is that the BACHD line may have deficits in the light-response of the circadian system and we carried out two additional experiments to test this possibility. First, we examined the ability of the BACHD mice to re-synchronize to 6 hr shifts in the LD cycle (**Fig. 3A**). We found that the BACHD mice took longer to resynchronize to both the 6 hr delay ($t_{13} = -2.25$, $P < 0.05$) and advance ($t_{13} = -3.11$, $P < 0.01$) in the LD cycle than their WT littermates. In addition, to directly assess the effects of light on the circadian system, the phase shifts induced by single, discrete light treatments were examined (**Fig. 3B**). Whereas WT littermates exposed to white light at CT 16 (100 lux, 10 min duration) showed a 113 ± 5 min ($n = 8$) phase delay, the BACHD mice had a 55% reduction in magnitude of phase delay after the same light treatment (51 ± 10 min, $n = 8$; $t_{15} = 5.53$, $P < 0.01$). Therefore, the circadian system of the BACHD mice shows a reduced sensitivity to the phase-shifting effect of light.

The distribution of behavioral sleep is disrupted in BACHD mice

To examine the sleep/wake temporal distribution, we measured behavioral sleep in young adult (3 mo) and middle aged (12 mo) BACHD mutants and their WT littermates (**Table 3**). Both mutants and WT mice showed significantly more daytime sleep at 12 mo than at 3 mo (two way ANOVA $F_{1,29} = 18.44$, $P < 0.001$), and the post-hoc Tukey's *t*-test revealed that the BACHD mutants had significantly less daytime sleep than WT at 3 mo of age ($t_{20} = 2.07$, $P = 0.049$). Nighttime sleep was significantly greater in 12 mo old WT mice than their younger counterparts ($t_{14} = 4.43$, $P < 0.001$), but this age-related effect was not observed in the BACHD mutants ($t_{12} = 0.14$, $P = 0.89$). A higher resolution analysis of sleep distribution of the 3 mo old BACHD mutants pinpointed the early hours of the day as the time during which they displayed markedly less sleep than the WT littermates (**Supp. Fig. 1**; two way repeated measures ANOVA $F_{7,20} = 2.82$, $P = 0.009$). Post-hoc analysis by Tukey's *t*-tests revealed that the BACHD mutants spent significantly less time in sleep during the hours of ZT 0 to ZT 3 ($t_{20} = 2.99$, $P = 0.003$) as well as between ZT 3 and ZT 6 ($t_{20} = 2.36$, $P = 0.02$). Therefore, the BACHD mice exhibited significantly reduced sleep during the early day.

Circadian rhythms of heart rate and body temperature are severely disrupted in the BACHD mice

Surgical implantation of a telemetric device into the abdomen of mice allows for continuous recording of ECG waveforms and body temperature in freely-moving WT and BACHD mice. We compared and analyzed a number of ECG features (RR, PR, QRS, QT, QTc intervals) between WT and BACHD mice under LD conditions to detect any diurnal and genotypic differences. Both the WT and BACHD mice displayed significant day/night differences in the RR, PR, and QRS (**Table 4**). Interestingly, the BACHD mice showed a significant increase in the PR interval during the night and a loss of diurnal rhythmicity in this parameter.

In order to examine the circadian component of HR and body temperature, we plotted the raw data to produce graphs similar to the actogram (**Fig. 4**) used for wheel-running activity analysis. We also analyzed the raw data of individual mice by periodogram analysis (**Table 5**) and used the amplitude as an index of rhythm strength. Under LD conditions, WT mice exhibited robust daily rhythms of HR and body temperature that were synchronized to the LD cycle. Significant diurnal differences in HR (t_6=−11.54, $P < 0.001$, $n = 7$) and body temperature (t_6=−8.693, $P < 0.001$, $n = 7$) were detected by *t*-tests (**Table 5**). When WT mice were placed in DD, circadian rhythms of HR and body temperature remained robust with a free-running period of 23.7 hrs (**Fig. 4, Table 5**). Circadian differences in average HR (t_6=9.085, $P < 0.001$, $n = 7$) and body temperature (t_6=−19.684, $P < 0.001$, $n = 7$) remained significant (**Table 5**). The BACHD mice displayed weak diurnal rhythms in HR and body temperature (**Fig. 4**). The mutant mice exhibited increased HR and temperature during the day compared to WT (**Table 5**). Furthermore, under DD conditions, we detected significant circadian differences in body temperature (t_7=−6.693, $P < 0.001$, $n = 8$) and HR (t_7=−3.636, $P = 0.008$, $n = 8$; **Table 5**). Under DD conditions, the average HR and body temperature was higher in the BACHD mice than in WT (**Table 5**). These data indicate that the amplitude of the temporal patterning of HR and body temperature is reduced in the BACHD mice due to a higher HR and body temperature during the day.

Rhythms of HRV are disrupted in the BACHD mice

HRV is an index of the balance of sympathovagal signals to the heart and measures the variability of the time between individual heartbeats (Massin, et al., 2000). We assessed the temporal patterning of neural signals to the heart by calculating HRV from WT and BACHD mice under LD and DD conditions (**Fig. 5**). WT mice exhibited significant diurnal differences in HRV under LD (WT: t_4=3.00, $P = 0.04$) and significant circadian differences under DD conditions (t_4=3.582, $P = 0.023$). BACHD mice did not exhibit a diurnal difference in HRV under LD conditions (t_5=1.414, $P = 0.216$) or DD conditions (t_5=3.542, $P = 0.14$). The average HRV (measured over 24 hrs) was significantly lower in the BACHD group ($t_{10} = 2.511$, $P = 0.031$, **Fig. 5**). Overall our data suggest that the autonomic system is still functioning but the temporal patterning is altered, with particular deficits in the daytime or rest phase. These results suggest that temporal patterning as well as the overall level of autonomic regulation of the cardiovascular system is compromised in the BACHD mice.

Daytime excitability of SCN neurons is reduced in the BACHD mice

Using the current-clamp recording technique in the whole-cell patch clamp configuration (**Fig. 6**), we measured the SFR in dorsal SCN neurons from WT (n = 25) and BACHD (n = 26) mice. Recordings (1 min) were made during the day (ZT 4-6) and night (ZT 14-16) and the resulting data analyzed by twoway ANOVA. This analysis revealed a significant effect of time of day ($F_{1,50}$ = 94.23, P < 0.05). As expected, the SFR of WT mice was significantly (t = 4.395, P <0.05) higher during the day (6.7 ± 1.5 Hz, n = 13) than during the night (2.1 ± 0.7 Hz, n = 12). In contrast, in the BACHD mice, there were no significant (t = 0.836, P = 0.557) differences between SFR during the day (3.1 ± 0.8 Hz, n = 14) and night (2.3 ± 1.0 Hz, n = 12). The daytime SFR was significantly reduced (t = 3.575, P = 0.015) in the BACHD mice compared to WT mice. So the insertion of the human HD gene appeared to eliminate the day/night difference in spontaneous activity in the mouse SCN by reducing the firing rate during the day.

PER2 expression is not altered in the SCN of BACHD mice

To determine if the molecular machinery necessary to generate circadian oscillations was affected by the insertion of the HD gene, we used IHC to examine PER2 protein expression within the SCN. The wheel running activity of WT and BACHD mice in LD was monitored and the mice were placed in DD for 3 days. Mice (n = 3-4 per time point) from each genotype were sampled at 2 different points in the daily cycle (CT 2 and 14). PER2 was strongly expressed in the SCN of both WT and BACHD mice (**Fig. 7**) with immuno-reactivity seen throughout the SCN. The mean number of immuno-positive neurons per SCN section varied with time of day (**Fig. 7**) with peak counts found at early subjective night (CT 14) and low counts measured in the early subjective day (CT 2). As measured by the PER2 rhythm, we do not see any evidence for gross disruption of the molecular clockwork in the BACHD mutant mice.

Discussion

There are 3 general types of mouse models of HD (Cepeda, et al., 2010, Levine, et al., 2004, Menalled, et al., 2009) including: transgenic mice expressing the entire human HD gene (BACHD), transgenic mice expressing the first exon of the HD gene (R6/2), and knock-in mice generated by inserting the expanded CAG repeats into the mouse HD gene (CAG 140). No single mouse model can be expected to recapitulate all aspects of the human disease; therefore, we felt that it was important to explore possible circadian dysfunction in different mouse models of HD. First, we confirmed the dramatic loss of daily and circadian rhythms in the R6/2 line (CAG 240, and CAG 140) as has been reported by Dr. Morton and colleagues (**Fig. 1**; Morton, et al., 2005, Pallier, et al., 2007). Both of the R6/2 lines of mice quickly progressed from pre-symptomatic (4-6 weeks) to disrupted circadian rhythms and death (8-12 weeks). This rapid progression makes the R6/2 lines excellent models for many aspects of HD but also made examination of the circadian phenotype difficult. Many of the behavioral tests used to measure circadian parameters last longer than the short lifespan of the R6/2 mice. In contrast, the CAG 140 KI mice did not show a circadian phenotype at 3 mo of age (**Fig. 1**). At the older ages, the CAG 140 KI showed reduced amplitude locomotor activity rhythms (10-20%, P > 0.05) and increased time to reentrain to a shift in the LD

cycle (data not shown). However, the circadian effects were mild compared to that seen in the other models and we stopped collecting data when the mice were 12 mo of age. The mice line that we used was not fully back-crossed onto the C57 background, so the genetic background may have contributed to the mild circadian phenotype. Of course, the mice may well have developed a more significant circadian phenotype at an older age.

The BACHD line exhibited clear diurnal and circadian deficits in wheel running activity at 3 mo of age (**Fig. 1**), a time at which motor deficits associated with the HD phenotype are first seen in this mouse model, but prior to development of neurodegeneration (Gray, et al., 2008). There was a clear age-related progression to the disease with the amplitude of the rhythms declining with age (**Fig. 2**). The central clock driving circadian rhythms is located in the SCN in the hypothalamus. While many of the symptoms of HD appear to be the result of pathology within the basal ganglia, there has long been evidence that hypothalamic dysfunction is also involved (Kremer, et al., 1990, Lavin, et al., 1981, Petersén, et al., 2005, Wood, et al., 2008). In humans, many of the non-motor symptoms of HD begin before the onset of motor symptoms, and include dysfunctions in hypothalamic-driven function, such as sleep, emotional state and metabolism (Duff, et al., 2007, Julien, et al., 2007, Soneson, et al., 2010). The early onset of the circadian disorders described in the present study (3 mo or young adult) fits with the clinical disease progression seen in humans. Besides a clear deficit in the behavioral output, we were also able to document a compromised light response of the BACHD mice (**Fig. 3**). The mice had difficulty adjusting to changes in the LD cycle, possibly due to the decreased magnitude of the phase shifting effects of light. One likely consequence of these entrainment deficits is that the BACHD mice exhibit more activity during the time of the daily LD cycle when they should be sleeping. In HD patients, sleep disturbances are a common clinical complaint that impairs the quality of life (Goodman and Barker, 2010). To explore the sleep/wake patterns of the BACHD, we turned to behavioral measures of sleep (Campbell and Tobler, 1984, Loh, et al., 2010, Schwartz and Smale, 2005). We measured the patterns of sleep/wake in BACHD and WT littermates using video analysis. The results (**Table 3**) clearly show that the mice exhibited a reduction of sleep early in their sleep cycle. This observation with the BACHD mice parallels clinical observations of a prolonged sleep latency in the HD patients (Aziz, et al., 2010, Cuturic, et al., 2009, Goodman and Barker, 2010). Future work using EEG recordings will be necessary to specifically examine if the BACHD mice show any change in sleep states or in the depth of sleep.

In HD patients, there is the suggestion of cardiac dysfunction with the best evidence indicating that HD alters the autonomic tone in cardiac tissue (e.g. Andrich, et al., 2002, Bär, et al., 2008, Kobal, et al., 2004). The telemetry system enabled us to record ECG waveforms (**supplemental Fig. 2**) and calculate HRV from WT and BACHD mice under LD and DD conditions. HRV is a measure of the variation in the beat-to-beat (R-R) interval, and reflects the balance of sympathetic and parasympathetic input to the heart. We found an overall decrease in HRV in BACHD mice compared to WT mice, indicating autonomic dysfunction in the BACHD mice (**Fig. 5**). A decrease in HRV has been previously reported in patients in the early presymptomatic and middle stages of HD progression (Andrich, et al., 2002, Kobal, et al., 2010). As both HR and body temperature are regulated by the autonomic

nervous system (ANS), the increase in average HR and body temperature observed in BACHD mice compared to WT mice is further evidence for dysfunction of the ANS. It is interesting to consider that the telemetry recordings were carried out without the presence of a running wheel which can alter overall activity levels in mice. Reduced HRV is generally considered an indication of poor cardiovascular health and has been shown to be a predictor for cardiovascular disease and mortality (Bigger, et al., 1992, Buccelletti, et al., 2009, Thayer, et al., 2010). In this regard, it is worth considering that the autonomic imbalance may be promoting cardiac failure, which is a leading cause of death among HD patients (Chiu and Alexander, 1982, Lanska, et al., 1988). In addition to the overall decrease of HRV, the diurnal and circadian rhythms of HRV were also lost in BACHD mice. The loss of rhythms in autonomic output and the shift in autonomic balance may be driving the damped rhythms of HR and body temperature in BACHD mice. We also compared various ECG parameters between WT and BACHD mice under LD conditions (**Table 4**). While most parameters were not different between the two genotypes and displayed significant day/night differences, we did not detect a day/night difference in the PR interval in the BACHD mice and the night-time value was increased compared to WT. The PR interval reflects the time the electrical impulse takes to travel from the sinus node through the atrioventricular node, the electrical pathway that connects the top chambers to the bottom chambers of the heart. Regulation of this interval is dependent upon a number of factors, one being input from the autonomic system, whereby the PR interval elongates with increased parasympathetic tone, and shortens with increased sympathetic tone (Carruthers, et al., 1987, Wallick, et al., 1982). Thus, the loss of day/night difference in the PR interval seen in the BACHD mice is further evidence for a dysfunction in ANS regulation. Overall, the dramatic decrease in HRV, increase in HR and body temperature, loss of day/night differences in the PR interval, as well as the decrease in the amplitude of rhythmicity in HR and body temperature suggests that the function of the ANS is compromised in the BACHD mice.

SCN neurons are spontaneously active neurons that generate AP with a peak frequency of around 10-12 Hz during the day (Ko, et al., 2009, Kuhlman and McMahon, 2006). During the night, SCN neurons are normally quiescent. In the present study, we examined the impact of the BACHD on the level of spontaneous activity during the day and night (**Fig. 6**). In the daytime, we found that the excitability of SCN neurons was significantly reduced in the BACHD mice. Neurons in the SCN are well positioned to drive the rhythms in cardiac output through the regulation of the ANS (Buijs, et al., 2003, Kalsbeek, et al., 2006). Previous anatomical studies have shown that VIP is expressed in SCN efferents projecting onto pre-autonomic neurons of the paraventricular nucleus (Teclemariam-Mesbah, et al., 1997). Both VIP message and protein are reduced in the SCN of R6/2 mice (Fahrenkrug, et al., 2007) suggesting a mechanism through which cardiac output may be altered in this line of mice. The decrease in the daytime electrical activity in the SCN could well weaken the temporal patterning of the ANS. The rhythms in both HR and body temperature were reduced in the BACHD mice due to deficits in the inhibition of these parameters in the day. Similarly, the induction of sleep was significantly reduced early in the day. These observations are all consistent with the hypothesis that the weakening of electrical output from the SCN could underlie a number of the phenotypes observed in the BACHD mice. These physiological results provide important support for the hypothesis that the HD

mutation alters the generation of the daily rhythms in firing rate that are a hallmark feature of SCN neurons.

Interacting molecular feedback loops driving rhythmic transcription and translation of key clock genes such as *Period* (e.g. Hastings, et al., 2003) are at the core of the oscillatory mechanism responsible for driving circadian oscillation. As a first screen for possible deficits in this molecular clockwork, we looked at PER2 expression in the peak and trough of the rhythm (**Fig. 7**). By this measure, we do not see any evidence that the molecular clockwork is disrupted in the SCN of BACHD mutant mice. However, in light of the differential loss of rhythms in the core clock genes Cry1 and Dbp, but not of Bmal1 and Per2 in the liver of R6/2 mice (Maywood et al., 2010), further work is required for a definitive answer as to whether rhythms in gene expression are altered in the SCN of BACHD mice. Prior work with the R6/2 line suggests that the behavioral impairment in the mice is accompanied by disordered expression of circadian clock genes *in vivo* in the hypothalamus (SCN) and in the motor controls regions of the brain including the striatum (Pallier, et al., 2007). The BACHD mice did show a lengthening of free-running period in DD (**Table 1**). Changes in the circadian period length are indicative of a disruption in the underlying circadian pacemaker system (Takahashi, et al., 2008). Therefore, our data with the BACHD mice suggest that these mice have deficits in all of the key elements of the circadian timing system including photic input, generation of oscillations, and outputs.

This disruption of circadian rhythms is likely to have profound consequences on the health of the HD patient (Hastings, et al., 2003; Takahashi, et al., 2008). It is becoming increasing clear that robust daily rhythms of sleep & wake are essential to good health. A wide range of studies have demonstrated that disruption of the circadian system leads to a cluster of symptoms, including metabolic deficits (Marcheva, et al., 2010, Turek, et al., 2005), cardiovascular problems (Bray, et al., 2008, Feng, et al., 2006), difficulty sleeping (Reid and Zee, 2009, Wulff, et al., 2009) and cognitive deficits (Gerstner, et al., 2009, Loh, et al., 2010, Wang, et al., 2009). Many of these same symptoms are seen in HD patients prior to onset of motor symptoms. This brings up the question as to the extent that circadian perturbations exacerbate the non-motor symptoms of HD. Recent work suggests that interventions that may stabilize the deteriorating daily rhythms can help with the cognitive symptoms in the R6/2 line (Maywood, et al., 2010, Pallier, et al., 2007). We do not know yet if these interventions actually improve the circadian rhythms and if this type of treatment strategy can be effective in mouse models. Based on the present data, future work will need to focus on a better understanding of how the BACHD mutation alters the electrical activity within the SCN and on interventions that can improve these disruptions.

Supplementary Material

Refer to Web version on PubMed Central for supplementary material.

Acknowledgments

This work was supported by the CHDI Foundation, the Oppenheimer Foundation and the American Heart Association. We would also like to thank Ms. Donna Crandall for assistance with the graphics.

Abbreviations

ANOVA	analysis of variance
ANS	autonomic nervous system
CT	circadian time
DD	constant darkness
ECG	electrocardiogram
HD	Huntington's disease
HR	heart rate
HRV	heart rate variability
IHC	immunohistochemistry
LD	light-dark
PER2	PERIOD2
SCN	suprachiasmatic nucleus
VIP	vasoactive intestinal peptide
WT	wild-type
ZT	zeitgeber time

References

1. Andrich J, Schmitz T, Saft C, Postert T, Kraus P, Epplen J, Przuntek H, Agelink M. Autonomic nervous system function in Huntington's disease. J Neurol Neurosurg Psychiatry. 2002; 72:726–731. [PubMed: 12023413]
2. Aziz N, Anguelova G, Marinus J, Lammers G, Roos R. Sleep and circadian rhythm alterations correlate with depression and cognitive impairment in Huntington's disease. Parkinsonism Relat Disord. 2010; 16:345–350. [PubMed: 20236854]
3. Bigger JJ, Fleiss J, Steinman R, Rolnitzky L, Kleiger R, Rottman J. Frequency domain measures of heart period variability and mortality after myocardial infarction. Circulation. 1992; 85:164–171. [PubMed: 1728446]
4. Bray M, Shaw C, Moore M, Garcia R, Zanquetta M, Durgan D, Jeong W, Tsai J, Bugger H, Zhang D, Rohrwasser A, Rennison J, Dyck J, Litwin S, Hardin P, Chow C, Chandler M, Abel E, Young M. Disruption of the circadian clock within the cardiomyocyte influences myocardial contractile function, metabolism, and gene expression. Am J Physiol Heart Circ Physiol. 2008; 294:H1036–1047. [PubMed: 18156197]
5. Buccelletti E, Gilardi E, Scaini E, Galiuto L, Persiani R, Biondi A, Basile F, Silveri N. Heart rate variability and myocardial infarction: systematic literature review and metanalysis. Eur Rev Med Pharmacol Sci. 2009; 13:299–307. [PubMed: 19694345]
6. Buijs R, la Fleur S, Wortel J, Van Heyningen C, Zuiddam L, Mettenleiter T, Kalsbeek A, Nagai K, Niijima A. The suprachiasmatic nucleus balances sympathetic and parasympathetic output to peripheral organs through separate preautonomic neurons. J Comp Neurol. 2003; 464:36–48. [PubMed: 12866127]
7. Bär K, Boettger M, Andrich J, Epplen J, Fischer F, Cordes J, Koschke M, Agelink M. Cardiovagal modulation upon postural change is altered in Huntington's disease. Eur J Neurol. 2008; 15:869–871. [PubMed: 18484985]

8. Campbell SS, Tobler I. Animal sleep: a review of sleep duration across phylogeny. Neurosci Biobehav Rev. 1984; 8:269–300. [PubMed: 6504414]
9. Carruthers S, McCall B, Cordell B, Wu R. Relationships between heart rate and PR interval during physiological and pharmacological interventions. Br J Clin Pharmacol. 1987; 23:259–265. [PubMed: 2882775]
10. Cepeda C, Cummings D, André V, Holley S, Levine M. Genetic mouse models of Huntington's disease: focus on electrophysiological mechanisms. ASN Neuro. 2010; 2:e00033. [PubMed: 20396376]
11. Chiu E, Alexander L. Causes of death in Huntington's disease. Med J Aust. 1982; 1:153. [PubMed: 6210834]
12. Colwell C, Michel S, Itri J, Rodriguez W, Tam J, Lelievre V, Hu Z, Liu X, Waschek J. Disrupted circadian rhythms in VIP- and PHI-deficient mice. Am J Physiol Regul Integr Comp Physiol. 2003; 285:R939–949. [PubMed: 12855416]
13. Colwell C, Michel S, Itri J, Rodriguez W, Tam J, Lelièvre V, Hu Z, Waschek J. Selective deficits in the circadian light response in mice lacking PACAP. Am J Physiol Regul Integr Comp Physiol. 2004; 287:R1194–1201. [PubMed: 15217792]
14. Cuturic M, Abramson R, Vallini D, Frank E, Shamsnia M. Sleep patterns in patients with Huntington's disease and their unaffected first-degree relatives: a brief report. Behav Sleep Med. 2009; 7:245–254. [PubMed: 19787493]
15. Dragich J, Loh D, Wang L, Vosko A, Kudo T, Nakamura T, Odom I, Tateyama S, Hagopian A, Waschek J, Colwell C. The role of the neuropeptides PACAP and VIP in the photic regulation of gene expression in the suprachiasmatic nucleus. Eur J Neurosci. 2010; 31:864–875. [PubMed: 20180841]
16. Duff K, Paulsen J, Beglinger L, Langbehn D, Stout J, Group, P.-H. I. o. t. H. S. Psychiatric symptoms in Huntington's disease before diagnosis: the predict-HD study. Biol Psychiatry. 2007; 62:1341–1346. [PubMed: 17481592]
17. Fahrenkrug J, Popovic N, Georg B, Brundin P, Hannibal J. Decreased VIP and VPAC2 receptor expression in the biological clock of the R6/2 Huntington's disease mouse. J Mol Neurosci. 2007; 31:139–148. [PubMed: 17478887]
18. Feng J, Hu Y, Xie L, Colwell C, Shao X, Sun X, Chen B, Tang H, Campagnoni A. Golli protein negatively regulates store depletion-induced calcium influx in T cells. Immunity. 2006; 24:717–727. [PubMed: 16782028]
19. Gerstner JR, Lyons LC, Wright KP Jr. Loh DH, Rawashdeh O, Eckel-Mahan KL, Roman GW. Cycling behavior and memory formation. J Neurosci. 2009; 29:12824–12830. [PubMed: 19828795]
20. Goodman A, Barker R. How vital is sleep in Huntington's disease? J Neurol. 2010; 257:882–897. [PubMed: 20333394]
21. Gray M, Shirasaki D, Cepeda C, André V, Wilburn B, Lu X, Tao J, Yamazaki I, Li S, Sun Y, Li X, Levine M, Yang X. Full-length human mutant huntingtin with a stable polyglutamine repeat can elicit progressive and selective neuropathogenesis in BACHD mice. J Neurosci. 2008; 28:6182–6195. [PubMed: 18550760]
22. Hastings M, Reddy A, Maywood E. A clockwork web: circadian timing in brain and periphery, in health and disease. Nat Rev Neurosci. 2003; 4:649–661. [PubMed: 12894240]
23. Hickey M, Kosmalska A, Enayati J, Cohen R, Zeitlin S, Levine M, Chesselet M. Extensive early motor and non-motor behavioral deficits are followed by striatal neuronal loss in knock-in Huntington's disease mice. Neuroscience. 2008; 157:280–295. [PubMed: 18805465]
24. Itri J, Michel S, Vansteensel M, Meijer J, Colwell C. Fast delayed rectifier potassium current is required for circadian neural activity. Nat Neurosci. 2005; 8:650–656. [PubMed: 15852012]
25. Itri J, Vosko A, Schroeder A, Dragich J, Michel S, Colwell C. Circadian Regulation of A-type Potassium Currents in the Suprachiasmatic Nucleus. J Neurophysiol. 2009
26. Julien C, Thompson J, Wild S, Yardumian P, Snowden J, Turner G, Craufurd D. Psychiatric disorders in preclinical Huntington's disease. J Neurol Neurosurg Psychiatry. 2007; 78:939–943. [PubMed: 17178819]

27. Kalsbeek A, Perreau-Lenz S, Buijs R. A network of (autonomic) clock outputs. Chronobiol Int. 2006; 23:521–535. [PubMed: 16753939]
28. Ko G, Shi L, Ko M. Circadian regulation of ion channels and their functions. J Neurochem. 2009; 110:1150–1169. [PubMed: 19549279]
29. Kobal J, Meglic B, Mesec A, Peterlin B. Early sympathetic hyperactivity in Huntington's disease. Eur J Neurol. 2004; 11:842–848. [PubMed: 15667417]
30. Kobal J, Melik Z, Cankar K, Bajrovic F, Meglic B, Peterlin B, Zaletel M. Autonomic dysfunction in presymptomatic and early symptomatic Huntington's disease. Acta Neurol Scand. 2010; 121:392–399. [PubMed: 20047567]
31. Kremer H, Roos R, Dingjan G, Marani E, Bots G. Atrophy of the hypothalamic lateral tuberal nucleus in Huntington's disease. J Neuropathol Exp Neurol. 1990; 49:371–382. [PubMed: 2141871]
32. Kuhlman S, McMahon D. Encoding the ins and outs of circadian pacemaking. J Biol Rhythms. 2006; 21:470–481. [PubMed: 17107937]
33. Lanska D, Lavine L, Lanska M, Schoenberg B. Huntington's disease mortality in the United States. Neurology. 1988; 38:769–772. [PubMed: 2966305]
34. Lavin P, Bone I, Sheridan P. Studies of hypothalamic function in Huntington's chorea. J Neurol Neurosurg Psychiatry. 1981; 44:414–418. [PubMed: 6455503]
35. Levine M, Cepeda C, Hickey M, Fleming S, Chesselet M. Genetic mouse models of Huntington's and Parkinson's diseases: illuminating but imperfect. Trends Neurosci. 2004; 27:691–697. [PubMed: 15474170]
36. Loh D, Navarro J, Hagopian A, Wang L, Deboer T, Colwell C. Rapid changes in the light/dark cycle disrupt memory of conditioned fear in mice. PLoS One. 2010; 5
37. Mangiarini L, Sathasivam K, Seller M, Cozens B, Harper A, Hetherington C, Lawton M, Trottier Y, Lehrach H, Davies S, Bates G. Exon 1 of the HD gene with an 20 expanded CAG repeat is sufficient to cause a progressive neurological phenotype in transgenic mice. Cell. 1996; 87:493–506. [PubMed: 8898202]
38. Marcheva B, Ramsey K, Buhr E, Kobayashi Y, Su H, Ko C, Ivanova G, Omura C, Mo S, Vitaterna M, Lopez J, Philipson L, Bradfield C, Crosby S, JeBailey L, Wang X, Takahashi J, Bass J. Disruption of the clock components CLOCK and BMAL1 leads to hypoinsulinaemia and diabetes. Nature. 2010; 466:627–631. [PubMed: 20562852]
39. Massin M, Maeyns K, Withofs N, Ravet F, Gérard P. Circadian rhythm of heart rate and heart rate variability. Arch Dis Child. 2000; 83:179–182. [PubMed: 10906034]
40. Maywood E, Fraenkel E, McAllister C, Wood N, Reddy A, Hastings M, Morton A. Disruption of peripheral circadian timekeeping in a mouse model of Huntington's disease and its restoration by temporally scheduled feeding. J Neurosci. 2010; 30:10199–10204. [PubMed: 20668203]
41. Menalled L, El-Khodor B, Patry M, Suárez-Fariñas M, Orenstein S, Zahasky B, Leahy C, Wheeler V, Yang X, MacDonald M, Morton A, Bates G, Leeds J, Park L, Howland D, Signer E, Tobin A, Brunner D. Systematic behavioral evaluation of Huntington's disease transgenic and knock-in mouse models. Neurobiol Dis. 2009; 35:319–336. [PubMed: 19464370]
42. Menalled L, Sison J, Dragatsis I, Zeitlin S, Chesselet M. Time course of early motor and neuropathological anomalies in a knock-in mouse model of Huntington's disease with 140 CAG repeats. J Comp Neurol. 2003; 465:11–26. [PubMed: 12926013]
43. Morton A, Wood N, Hastings M, Hurelbrink C, Barker R, Maywood E. Disintegration of the sleep-wake cycle and circadian timing in Huntington's disease. J Neurosci. 2005; 25:157–163. [PubMed: 15634777]
44. Pack A, Galante R, Maislin G, Cater J, Metaxas D, Lu S, Zhang L, Von Smith R, Kay T, Lian J, Svenson K, Peters L. Novel method for high-throughput phenotyping of sleep in mice. Physiol Genomics. 2007; 28:232–238. [PubMed: 16985007]
45. Pallier P, Maywood E, Zheng Z, Chesham J, Inyushkin A, Dyball R, Hastings M, Morton A. Pharmacological imposition of sleep slows cognitive decline and reverses dysregulation of circadian gene expression in a transgenic mouse model of Huntington's disease. J Neurosci. 2007; 27:7869–7878. [PubMed: 17634381]

46. Petersén A, Gil J, Maat-Schieman M, Björkqvist M, Tanila H, Araújo I, Smith R, Popovic N, Wierup N, Norlén P, Li J, Roos R, Sundler F, Mulder H, Brundin P. Orexin loss in Huntington's disease. Hum Mol Genet. 2005; 14:39–47. [PubMed: 15525658]
47. Reid K, Zee P. Circadian rhythm disorders. Semin Neurol. 2009; 29:393–405. [PubMed: 19742414]
48. Schroeder A, Loh D, Jordan M, Roos K, Colwell C. Circadian Regulation of Cardiovascular Function: a role for vasoactive intestinal peptide. Am J Physiol Heart Circ Physiol. 2010 Epub Oct 15.
49. Schwartz M, Smale L. Individual differences in rhythms of behavioral sleep and its neural substrates in Nile grass rats. J Biol Rhythms. 2005; 20:526–537. [PubMed: 16275771]
50. Soneson C, Fontes M, Zhou Y, Denisov V, Paulsen J, Kirik D, Petersén A, investigators, T. H. S. G. P.-H. Early changes in the hypothalamic region in prodromal Huntington disease revealed by MRI analysis. Neurobiol Dis. 2010
51. Takahashi J, Hong H, Ko C, McDearmon E. The genetics of mammalian circadian order and disorder: implications for physiology and disease. Nat Rev Genet. 2008; 9:764–775. [PubMed: 18802415]
52. Teclemariam-Mesbah R, Kalsbeek A, Pevet P, Buijs R. Direct vasoactive intestinal polypeptide-containing projection from the suprachiasmatic nucleus to spinal projecting hypothalamic paraventricular neurons. Brain Res. 1997; 748:71–76. [PubMed: 9067446]
53. Thayer J, Yamamoto S, Brosschot J. The relationship of autonomic imbalance, heart rate variability and cardiovascular disease risk factors. Int J Cardiol. 2010; 141:122–131. [PubMed: 19910061]
54. The Huntington's Disease Collaborative Research Group. A novel gene containing a trinucleotide repeat that is expanded and unstable on Huntington's disease chromosomes. Cell. 1993; 72:971–983. [PubMed: 8458085]
55. Turek F, Joshu C, Kohsaka A, Lin E, Ivanova G, McDearmon E, Laposky A, Losee- Olson S, Easton A, Jensen D, Eckel R, Takahashi J, Bass J. Obesity and metabolic syndrome in circadian Clock mutant mice. Science. 2005; 308:1043–1045. [PubMed: 15845877]
56. Wallick D, Martin P, Masuda Y, Levy M. Effects of autonomic activity and changes in heart rate on atrioventricular conduction. Am J Physiol. 1982; 243:H523–527. [PubMed: 7124960]
57. Wang L, Dragich J, Kudo T, Odom I, Welsh D, O'Dell T, Colwell C. Expression of the circadian clock gene Period2 in the hippocampus: possible implications for synaptic plasticity and learned behaviour. ASN Neuro. 2009; 1
58. Wood N, Goodman A, van der Burg J, Gazeau V, Brundin P, Björkqvist M, Petersén A, Tabrizi S, Barker R, Morton A. Increased thirst and drinking in Huntington's disease and the R6/2 mouse. Brain Res Bull. 2008; 76:70–79. [PubMed: 18395613]
59. Wulff K, Porcheret K, Cussans E, Foster R. Sleep and circadian rhythm disturbances: multiple genes and multiple phenotypes. Curr Opin Genet Dev. 2009; 19:237–246. [PubMed: 19423332]

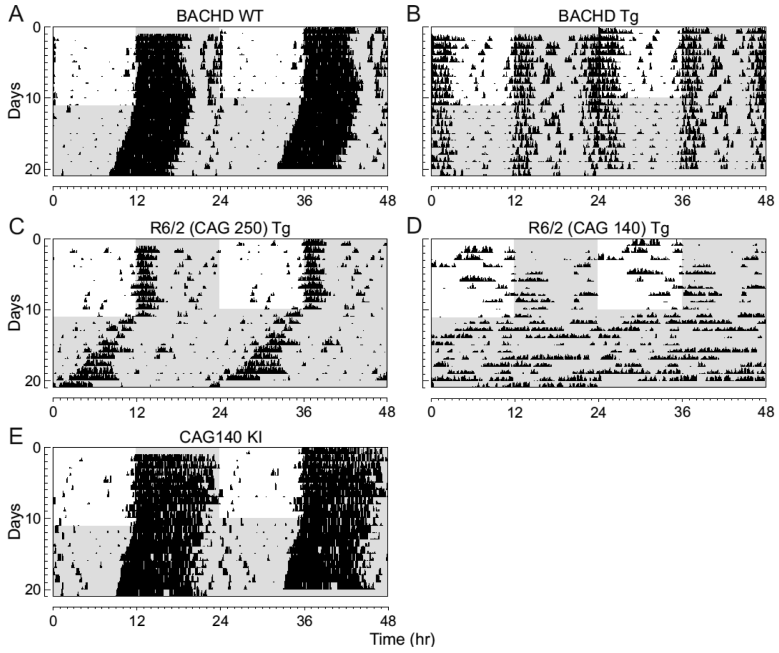

Fig. 1.

Circadian dysfunction is a common feature of mouse models of HD. Mice were placed individually in cages with running wheels, and locomotor activity was recorded under different lighting conditions. Each horizontal row represents an activity record for a 24-hr day. Successive days are plotted from top to bottom. The grey shading represents darkness. Mice were initially held in LD (12:12) and then released into DD. Panels show examples of the wheel-running activity recorded from WT (A), BACHD (B) , R6/2 CAG 250 (C), R6/2 CAG 140 (D), and CAG 140 (E). The mice were all 2-3 mo of age. See Table 1 for detailed analysis.

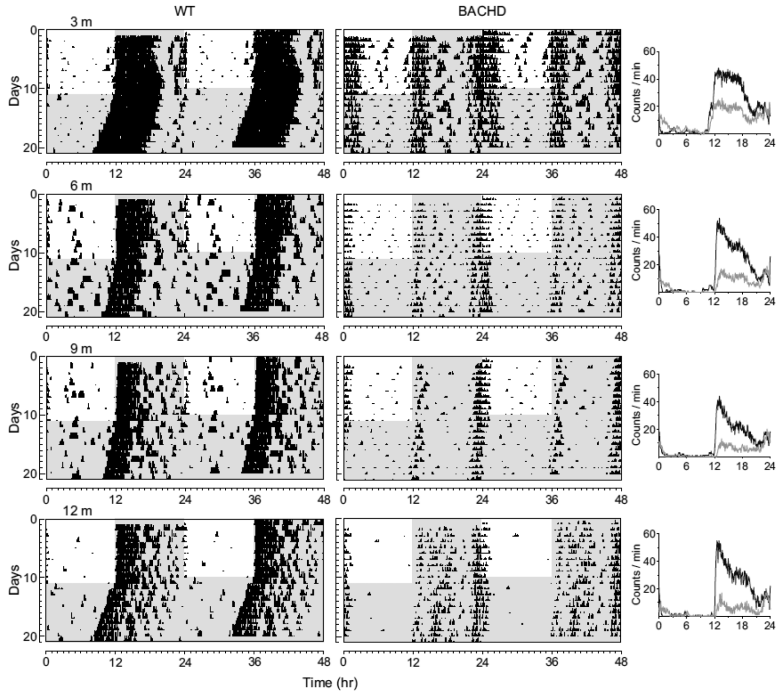

Fig. 2.

BACHD mice show an age-related decline in activity levels. Panels show examples of wheel-running activity measured from WT (left panels) and littermate BACHD (middle panels) measured at ~3, 6, 9, and 12 mo of age. The average waveform of activity for each genotype (black line =WT; grey line = BACHD) as measured over 10-days in LD is also shown (right panels). Activity and power showed progressive declines under both LD and DD conditions. See Table 2 for detailed analysis.

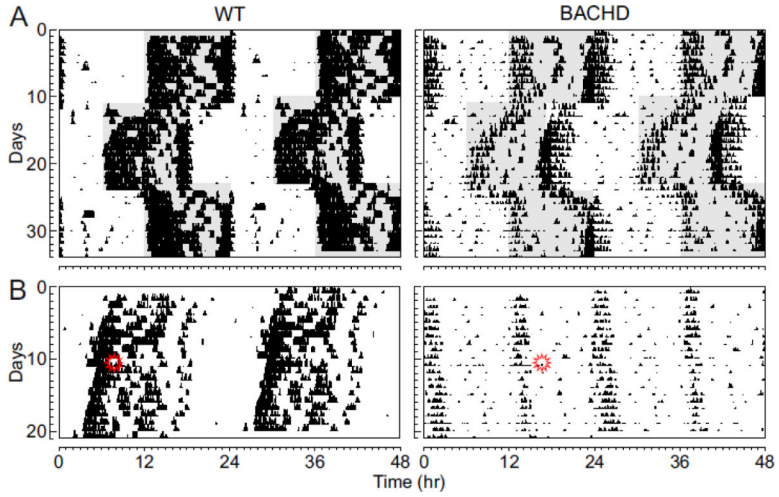

Fig. 3.

BACHD mice show a decreased circadian response to light. (A) Examples of the response to 6 hr shifts in the LD cycle for WT and BACHD mice at ~6 mo of age. (B) Examples of light-induced phase shifts for WT and BACHD mice at ~6 mo of age in DD. Mice in DD were exposed to light (100 lux, 10 min duration) at CT 16 (indicated by symbol) and the resulting phase delay measured.

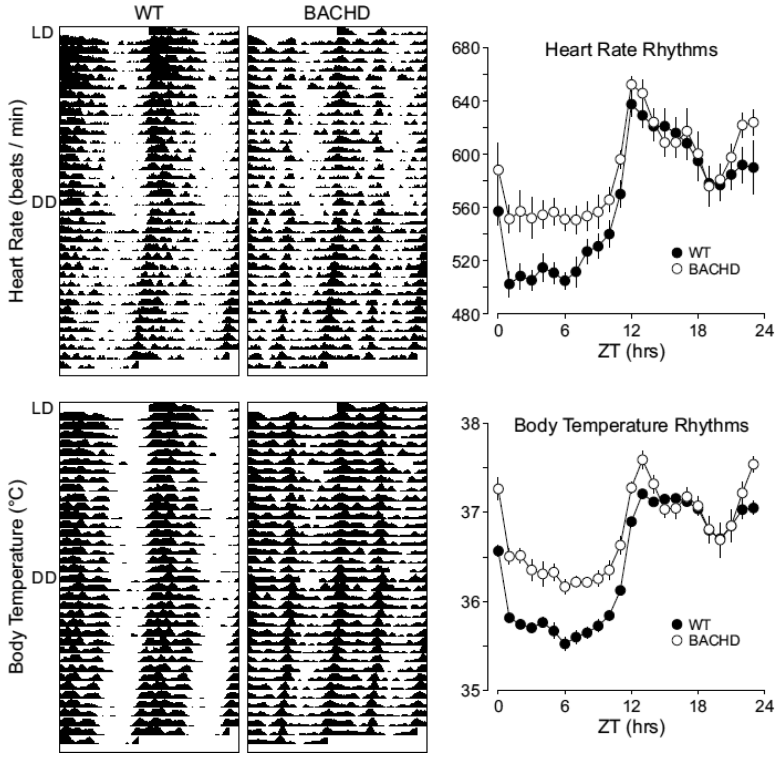

Fig. 4.

BACHD mice exhibit a breakdown in circadian rhythms as measured by telemetry. Examples of heart rate and body temperature measured from WT (left panels) and littermate BACHD (right panels) mice at ~6 mo of age are shown. Each horizontal row represents an activity record for a 24-hr day. Activity double plotted to aid detection of activity patterns. Successive days are plotted from top to bottom. The average waveform of activity for each genotype as measured over 10-days in LD is also shown (right panels).

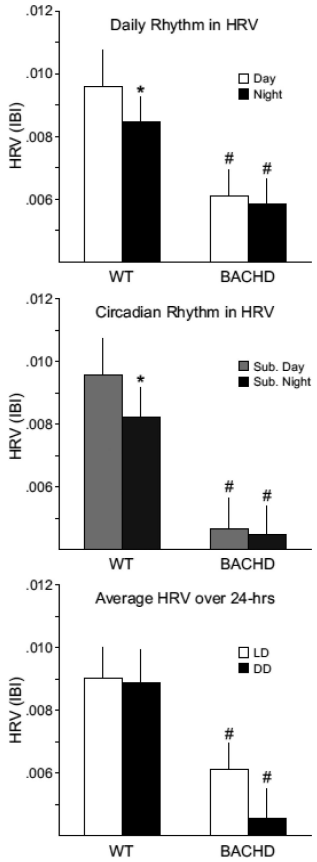

Fig. 5.

BACHD mice exhibit a loss of their circadian rhythm in HRV. HRV is determined by calculating the variance of the time between individual beats, and is also known as the inter-beat-interval (IBI). Top panel shows the average HRV as measured in the day and in the night when mice are maintained on an LD cycle. The middle panel shows the average HRV as measured in the subjective day and night under DD conditions. The bottom panel shows that the overall HRV was significantly reduced in the BACHD mice. The * indicates significance difference in the HRV at the level of $P < 0.05$ as analyzed by one-way ANOVA followed by Tukey's post-hoc comparison.

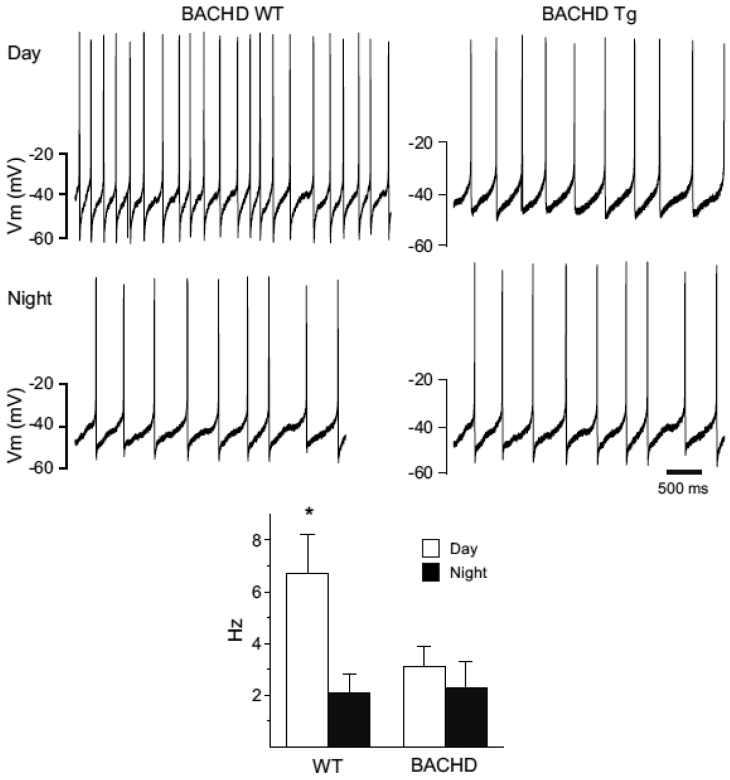

Fig. 6.

Daytime spontaneous neural activity is reduced in the SCN of BACHD mice. Using the current-clamp recording technique in the cell-attached configuration, we measured the spontaneous firing rate (SFR) in dorsal SCN neurons during the day (ZT 4-6; *n* = 13-14 per genotype) and night (ZT 16-18; *n* = 12 per genotype). The top panels show representative examples of firing rate recorded from the WT and BACHD mice at each time point. The bottom panel shows plots of average firing rate for each genotype. Data is shown at means ± SEM. The * indicates significance difference between SFR at the level of $P < 0.05$ as analyzed by two-way ANOVA followed by Tukey's post-hoc comparison.

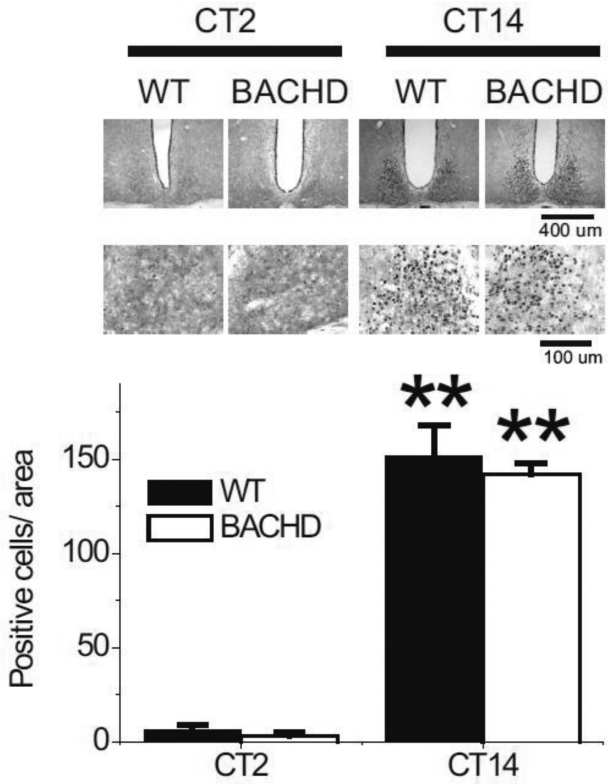

Fig. 7.

PER2 rhythm within the SCN did not appear to be disrupted even in aged BACHD mice. Mice were held in DD and wheel running activity measured to determine circadian phase. IHC was used to measure PER2 immunoreactivity in the SCN (n = 3-4 per group) of BACHD and WT controls. Tissue was collected in subjective day (CT 2) or subjective night (CT 14). (top panels) Photomicrographs of SCN tissue of each genotype in low (10X) and higher (40X) magnification. (bottom panel) Numbers of PER2 immuno-positive cells in the SCN varied as a function of time of day with highest count in early night. No differences were found between the genotypes. Tukey's post-hoc comparison, $^{**}P<0.01$ (vs. CT2).

Table 1

Key circadian parameters in 4 mouse models of HD.

Genotype:	WT	BACHD	R6/2 250	R6/2 140	CAG140 KI
LD					
Arrhythmic (%)	0 %	0 %	50 %	75 %	0 %
Power (% variation)	59.5±2.7	34.5±3.7**	na	na	52.9±4.6
Activity (rev/h)	981±70	628±99**	104±39**	195±125*	835±99
DD					
Arrhythmic (%)	0 %	0 %	50 %	75 %	0 %
Tau (hrs)	23.69±0.05	24.07±0.04*	na	na	23.82±0.04
Power (% variation)	50.8±5.5	31.0±4.3**	na	na	54.6±4.3
Activity (rev/h)	1050±34	543±121**	98±50**	195±98*	711±144

The mice (n = 4-8 per group) were all young adult (2-3 mo of age) males. Rhythms in wheel-running activity were examined using periodogram analysis. Comparisons were made between littermate WT and mutant mice with a Student's Z-Test with

* indicating a significant difference at $P < 0.05$

** indicating a significant difference at $P < 0.01$. In the R6/2 lines, the number of rhythmic animals was too low to accurately describe the circadian parameters. These parameters are labeled as not available (na).

Table 2

Age-related decline in amplitude of wheel-running activity rhythms in BACHD mice.

Genotype:	WT	BACHD
LD		
Power (% variation)		
3 mo	59.5±2.7	34.5±3.7*
6 mo	55.1±3.3	42.4±2.9*
9 mo	54.3±3.3	32.9±3.6*
12 mo	55.0±2.0	32.8±3.5*
Activity (rev/h)		
3 mo	981±70	628±99*
6 mo	713±73	297±52*#
9 mo	760±127	277±47*#
12 mo	734±118	233±58*#
DD		
Tau (hrs)		
3 mo	23.69±0.05	24.07±0.04*
6 mo	23.61±0.12	24.05±0.04*
9 mo	23.54±0.08	24.12±0.06*
12 mo	23.69±0.06	23.96±0.02*
Power (% variation)		
3 mo	50.8±5.5	31.0±4.3*
6 mo	51.2±4.8	34.7±2.9*
9 mo	45.8±3.8	31.2±2.1*
12 mo	45.1±2.4	27.5±2.3*
Activity (rev/hr)		
3 mo	1050±34	543±121*
6 mo	872±149	265±50*
9 mo	749±165	229±49*
12 mo	762±98	190±19*#
Fragmentation (bouts/day)		
3 mo	4.4±0.4	7.4±0.8*
6 mo	4.5±0.9	7.3±0.8*
9 mo	5.1±0.6	7.2±0.8*
12 mo	5.0±0.2	8.1±0.4*

Genotype:	**WT**	**BACHD**
Bimodal (%)		
3 mo	0 %	37.5 %
6 mo	0 %	62.5 %
9 mo	0 %	66.7 %
12 mo	0 %	50 %

Rhythms in wheel-running activity in male mice (n = 4-8 per age-group) were examined using periodogram analysis. Comparisons between age and genotype were made between littermate WT and mutant mice with a 2-way ANOVA followed by Tukey's post hoc analysis with

*indicating a significant difference at $P < 0.05$ between genotypes within age

#indicating $P < 0.05$ between ages within genotype.

Table 3

The distribution of behavioral sleep is altered in the BACHD mice.

Genotype:	WT	BACHD
Sleep in Day (%)		
3 mo	66.67 ± 1.53	61.98 ± 1.68*
12 mo	74.48 ± 2.65#	72.98 ± 2.65#
Sleep in Night (%)		
3 mo	26.53 ± 1.59	28.19 ± 1.74
12 mo	40.63 ± 2.76#	28.65 ± 2.76*
Sleep bouts in Day		
3 mo	8.25 ± 0.36	8.03 ± 0.39
12 mo	9.13 ± 0.62	7.88 ± 0.62
Sleep bouts in Night		
3 mo	3.65 ± 0.40	4.13 ± 0.44
12 mo	6.50 ± 0.70#	4.13 ± 0.70*

Behavioral measurements of sleep were carried out using video analysis on mice of 3 months (n = 12 per genotype) and 12 months of age (n = 4 per genotype). Comparisons between age and genotype were made between littermate WT and mutant mice with a 2-way ANOVA followed by Tukey's post hoc analysis.

*indicates $P < 0.05$ between genotypes within age while

#indicates $P < 0.05$ between ages within genotype.

Table 4

Average duration of ECG features (RR, PR, QRS, QT and QTc intervals) in WT and BACHD mice under LD conditions.

Genotype:		WT	BACHD
RR (ms)	Day	125 ± 4	122 ± 7
	Night	99 ± 2.3*	107 ± 5*
PR (ms)	Day	38.1 ± 0.9	37.5 ± 0.6
	Night	34.8 ± 0.6*	36.9 ± 0.6#
QRS (ms)	Day	13.9 ± 0.3	13.7 ± 0.3
	Night	12.9 ± 0.4*	13.5 ± 0.3*
QT (ms)	Day	51.9 ± 1.1	51.9 ± 2.8
	Night	44.8 ± 1.9	46.6 ± 2.2*
QTc (ms)	Day	128 ± 1	128 ± 3
	Night	123 ± 2*	124 ± 2*

ECG intervals at two time points: day (ZT 2-4) and night (ZT 14-16) were calculated and averaged over 8 days.

* indicates significant difference in intervals between day and night ($P < 0.05$), which was analyzed by a paired Student's Z-Test.

# indicates significant difference in intervals between WT and BACHD mice ($P < 0.05$) and was analyzed using an unpaired Student's Z-test.

Table 5

Key circadian parameters in heart rate and body temperature measured in freely moving mice maintained in constant darkness.

	Heart rate	
Genotype:	**WT**	**BACHD**
Arrhythmic (%)	0 %	0 %
Tau (hrs)	23.83±0.04	23.85±0.03
Power (%)	28.0 ± 1	26.3 ± 3
Average (24 hr)	561 ± 7	586 ± 8*
Sub. Day (average)	520 ± 7	554 ± 9*
Sub. Night (average)	595 ± 7	611 ± 8

	Body Temperature	
Genotype:	**WT**	**BACHD**
Arrhythmic (%)	0%	0 %
Tau (hrs)	23.83±0.03	23.85±0.02
Power (%)	69.2 ± 2	64.2 ± 4
Average (24 hr)	36.3 ± 0.04	36.6 ± 0.09*
Sub. Day (average)	35.6 ± 0.07	35.9 ± 0.14*
Sub. Night (average)	36.9 ± 0.03	37.0 ± 0.11

The mice (n = 6-8 per group) were all young adult (6 months of age) males. Rhythms in HR and body temperature were measured using telemetry and examined using periodogram analysis. Comparisons were made between littermate WT and mutant mice with a Student's Z-Test, with

**indicating a significant difference at $P < 0.01$.

*indicating a significant difference at $P < 0.05$